Available online at www.cuijca.com

INTERNATIONAL JOURNAL OF COMPUTATIONAL ANALYSIS

Vol (1), No. (1), pp. 01-09

CITY UNIVERSITY INTERNATIONAL JOURNAL OF COMPUTATIONAL ANALYSIS

Analysis of Regression and Correlation of Entropy Generation of Nanofluid in the MHD Peristaltic Flow

Munawwar Ali Abbas[1,*], *Ibrahim Hussain*[2]

[1]*Department of Computer Science, University of Baltistan Skardu, Gilgit-Baltistan, Pakistan*
[2]*Department of Buisness Management, University of Baltistan Skardu, Gilgit-Baltistan, Pakistan*

Keywords:
Regression
Correlation
Magnetohydrodynamics
Nanofluid
Entropy Generation

A B S T R A C T

This study presents the mathematical model of entropy generation on MHD peristaltic wave of Nanofluid. The governing equations have been developed by the assumption of low Reynold's number and long wavelength approximation. The analytical solution has been obtained with the help of perturbation method. The expression of temperature profile, pressure distribution and friction forces are presented graphically for some significant parameters. Further, the results of correlation and regression between the entropy generation and some other parameters have been plotted. It is very important to find the sensitivity of each parameter on entropy generation. Findings of regression analysis show that 81% of the variability of entropy generation for magnetic parameter, 99% of the variability of entropy generation for Brownian motion parameter, 40% of the variability of entropy generation for Thermophoresis parameter and 100% of the variability of entropy generation for Brinkmann is accounted for by the variable *Iv*. Similarly, a decrease of 2.562 in entropy generation for the various values of the independent variable Magnetic parameter, an increase of 2.029 in entropy generation for the values of Brownian motion, an increase of 6.307 in entropy generation for Thermophoresis and 68.492 in entropy generation scores for Brinkmann on every one-unit increase in *Iv*.

1. Introduction

The use of heat transfer fluids is one of the technological applications of nanoparticles that hold enormous promise which containing suspensions of nanoparticles to confront cooling problems in the thermal systems. Due to the great demands placed upon the heat transfer fluids in terms of decreasing or increasing energy release to systems. A significance research work has been done by Choi and Eastman [1-2] that a mixture of nanoparticles and base fluid that such fluids were designated as "Nanofluid". He defined a liquid of ultra-fine particle with dia less than 100nm. In the field of thermal engineering and heat transfer nanofluid has always been an engrossing term. Peristalsis in the connection with nanofluid has various application such as in engineering, bio-sciences and industrial. Several theoretical and experimental attempts to this area have been contributed. Specially the works of Lathams and Shapiro et al. [3] play very important role in this direction. Similarly, because

* Corresponding author: E-mail address: *munawer.abbas@uobs.edu.pk*

of its multiple advantages, research findings on peristaltic flows have got wide application in industries, numerous attempts have been made to literature to explore this direction which can be viewed in the available reference [4-6].

Keeping in mind the above-aforementioned discussion, in any of these studies correlation and regression has not been investigated. Therefore, the aim of the present study is to investigate the correlation and regression of entropy generation of the MHD peristaltic flow of nanofluid with a porous medium. For this purpose, the study applies the situation of small Reynolds number and long wavelength and an analytical technique named as Homotopy Perturbation Method (HPM) is used to solve the simplified partial differential equations. Expression for temperature, concentration pressure and entropy generation have been obtained graphically. Based on entropy generation results, correlation and regression derived and explained the role of some pertinent parameters on entropy generation. Such kind of investigations can be much beneficial to find the sensitivity of each parameter on objective functions which are we considered as entropy generation in this model.

2. Mathematical Formulation

We present, modeling of the Peristaltic motion viscous, electrically conducting and incompressible nanofluid properties through a two-dimensional non- uniform channel with sinusoidal wave propagating towards down its walls. As it is mentioned in the Fig. (1) that cartesian coordinate system is taken in such a way that x axis is considered along with the center line in the direction of wave propagation and y is transverse to it. The B_0, a uniform external magnetic field is imposing along the y axis and the induced magnetic field is assumed to be negligible. The geometry of the wall surface is defined as,

$$H(\tilde{x},\tilde{t}) = \breve{a}\sin\frac{2\pi}{\lambda}\,(\tilde{x} - C\tilde{t}) + b(\breve{x}) \tag{1}$$

where

$$b(\tilde{x}) = b_0 + \mathrm{K}\tilde{x}$$

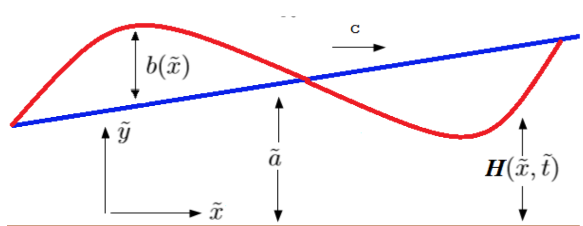

Figure 1. The geometry of the problem

The governing equation of motion, continuity, thermal energy and nano-particle fraction for peristaltic nanofluid can be written as [6].

$$\frac{\partial\tilde{u}}{\partial\tilde{x}} + \frac{\partial\tilde{v}}{\partial\tilde{y}} = 0, \tag{2}$$

$$\rho_f\left(\frac{\partial\tilde{u}}{\partial\tilde{t}} + \tilde{u}\frac{\partial\tilde{u}}{\partial\tilde{x}} + \tilde{v}\frac{\partial\tilde{u}}{\partial\tilde{y}}\right) = -\frac{\partial\tilde{p}}{\partial\tilde{x}} + \frac{\partial}{\partial\tilde{x}}\mathrm{S}_{\tilde{x}\tilde{x}} + \frac{\partial}{\partial\tilde{y}}\mathrm{S}_{\tilde{x}\tilde{y}} - \sigma B_0\tilde{u} - \frac{\mu}{k}\tilde{u} + g\begin{bmatrix}(1-F)\rho_{f_0}\zeta(T-T_0)\\ -(\rho_p - \rho_{f_0})(F-F_0)\end{bmatrix}, \tag{3}$$

$$\rho_f\left(\frac{\partial\tilde{v}}{\partial\tilde{t}} + \tilde{v}\frac{\partial\tilde{u}}{\partial\tilde{x}} + \tilde{v}\frac{\partial\tilde{v}}{\partial\tilde{y}}\right) = -\frac{\partial\tilde{p}}{\partial\tilde{y}} + \frac{\partial}{\partial\tilde{x}}\mathrm{S}_{\tilde{y}\tilde{x}} + \frac{\partial}{\partial\tilde{x}}\mathrm{S}_{\tilde{y}\tilde{y}} - \sigma B_0\tilde{v} - \frac{\mu}{k}\tilde{v} + g\begin{bmatrix}(1-F)\rho_{f_0}\zeta(T-T_0)\\ -(\rho_p - \rho_{f_0})(F-F_0)\end{bmatrix}, \tag{4}$$

$$(\rho c)_f\left(\frac{\partial T}{\partial\tilde{t}} + \tilde{u}\frac{\partial T}{\partial\tilde{x}} + \tilde{v}\frac{\partial T}{\partial\tilde{y}}\right) = \kappa\left(\frac{\partial^2 T}{\partial\tilde{x}^2} + \frac{\partial^2 T}{\partial\tilde{y}^2}\right) + (\rho c)_p\mathrm{D}_B\left(\frac{\partial T}{\partial\tilde{x}}\frac{\partial F}{\partial\tilde{x}} + \frac{\partial F}{\partial\tilde{y}}\frac{\partial T}{\partial\tilde{y}}\right) + \frac{\mathrm{D}_T}{T_0}\left(\left(\frac{\partial T}{\partial\tilde{x}}\right)^2 + \left(\frac{\partial T}{\partial\tilde{y}}\right)^2\right)$$

$$-\frac{\partial q_r}{\partial\tilde{y}} + Q_0, \tag{5}$$

$$\left(\frac{\partial F}{\partial \tilde{t}}+\tilde{u}\frac{\partial F}{\partial \tilde{x}}+\tilde{v}\frac{\partial F}{\partial \tilde{y}}\right)=\mathrm{D}_B\left(\frac{\partial^2 F}{\partial \tilde{x}^2}+\frac{\partial^2 F}{\partial \tilde{y}^2}\right)+\frac{\mathrm{D}_T}{T_0}\left(\frac{\partial^2 T}{\partial \tilde{x}^2}+\frac{\partial^2 T}{\partial \tilde{y}^2}\right)-k_1(F-F_0), \tag{6}$$

Now let us consider the assumptions of long wavelength number and low Reynolds approximations in the sense of creeping flow. By using dimensionless quantities in the Eq. (2) to Eq. (6), we get the resulting equations in a simplified form as

$$\frac{\partial^2 u}{\partial y^2}+We\frac{\partial}{\partial y}\left(\frac{\partial u}{\partial y}\right)^2-\frac{1}{k}u-M^2u-Gr_F\Phi+Gr_T\theta-\frac{\partial p}{\partial x}=0, \tag{7}$$

$$\left(\frac{1+\mathrm{R_n}}{\mathrm{Pr}}\right)\frac{\partial^2\theta}{\partial y^2}+N_t\left(\frac{\partial\theta}{\partial y}\right)^2+\beta+N_b\frac{\partial\theta}{\partial y}\frac{\partial\Phi}{\partial y}=0, \tag{8}$$

$$\frac{\partial^2\Phi}{\partial y^2}-\gamma\Phi+\frac{N_t}{N_b}\left(\frac{\partial^2\theta}{\partial y^2}\right)=0. \tag{9}$$

Subject to the respective boundary conditions

$$,\ \Phi(0)=0,\frac{\partial u(0)}{\partial y}=0,\ \theta(0)=0, \tag{10}$$

$$\Phi(h)=1,\theta(h)=1,\ u(h)=0 \tag{11}$$

In the presence of magnetic field, the entropy generation can be derived from energy and entropy balance for the case of heat and mass transfer as [8]

$$\mathrm{S_{gen}}=\frac{\mathcal{K}_{nf}}{T_0^2}(\nabla \mathrm{T})^2+\frac{\mu_{nf}}{\tilde{k}T_0}\begin{bmatrix}2\left(\frac{\partial\tilde{u}}{\partial\tilde{x}}\right)^2+2\left(\frac{\partial\tilde{v}}{\partial\tilde{y}}\right)^2\\ +\left(\frac{\partial\tilde{u}}{\partial\tilde{y}}+\frac{\partial\tilde{v}}{\partial\tilde{x}}\right)^2\end{bmatrix}+\frac{\sigma B_0^2}{T_0}\left(\frac{\partial\tilde{u}}{\partial\tilde{y}}\right)^2+\frac{R\mathrm{D_B}}{F_0}(\nabla F)^2+\frac{R\mathrm{D}_B}{T_0}(\nabla F\cdot\nabla T) \tag{12}$$

The dimensionless form of entropy generation number can be expressed as follows

$$N_s=\frac{\mathrm{S_{gen}}}{\mathrm{S_g}}=\left(\frac{\mathcal{K}_{nf}}{\mathcal{K}_f}\right)\left(\left(\frac{\partial\theta}{\partial y}\right)^2\right)+(1+M^2)B_r\frac{1}{\Omega}\left(\frac{\mu_{nf}}{\mu_f}\right)\left(\frac{\partial u}{\partial y}\right)^2+\Gamma\left(\frac{\Lambda}{\Omega}\right)^2\left(\frac{\partial\Phi}{\partial y}\right)^2+\ \zeta\left(\frac{\partial\theta}{\partial y}\right)\left(\frac{\partial\Phi}{\partial y}\right), \tag{13}$$

Where Ω, B_r, Λ, Γ, ζ are the dimensionless temperature difference, Brinkman number, concentration difference, diffusive coefficient and constant parameter are represented as

$$\Omega=\frac{(T_1-T_0)}{T_0},B_r=\frac{\tilde{c}^2\mu_f}{\tilde{k}\mathcal{K}_f(T_1-T_0)},\zeta=\frac{RD_BT_0}{\mathcal{K}_f}\left(\frac{F_1-F_0}{T_1-T_0}\right),\Gamma=\frac{R\mathrm{D}_BF_0}{\mathcal{K}_f},\Lambda=\frac{F_1-F_0}{F_0}. \tag{14}$$

For nanofluid, the viscosity model and thermal conductivity can be defined as [19]

$$\mu_{nf}=\frac{\mu_f}{(1-\bar{\phi})^{2.5}},\qquad \mathcal{K}_{\mathrm{nf}}=\frac{\kappa_p+2\kappa_f+2\bar{\phi}(\kappa_p-\kappa_f)}{\kappa_p+2\kappa_f-\bar{\phi}(\kappa_p-\kappa_f)}\kappa_f \tag{15}$$

here, $\boldsymbol{\kappa_f}$ and $\boldsymbol{\kappa_p}$, are the thermal conductivities of the nanofluid and nano-particle respectively.

3. Solution of the problem

Considering Eq. (7) to Eq. (9) and with the help of HPM [7] it can be written as:

$$\mathcal{H}(w,\tilde{q}) = (1-\acute{q})(L_1(w) - L_1(\overline{w}_0)) + \acute{q}\left(L_1(w) + We\frac{\partial}{\partial y}\left(\frac{\partial w}{\partial y}\right)^2 + Gr_T\Theta - Gr_F\vartheta - \frac{\partial p}{\partial x}\right), \tag{16}$$

$$\mathcal{H}(\Theta,\tilde{q}) = (1-\acute{q})(L_2(\Theta) - L_2(\overline{\Theta}_0)) + \acute{q}\left(L_2(\Theta) + \frac{\mathrm{Pr}}{1+\mathrm{R_n Pr}}\left(N_b\frac{\partial\vartheta}{\partial y}\frac{\partial\Theta}{\partial y} + N_t\left(\frac{\partial\vartheta}{\partial y}\right)^2\right) + \frac{\mathrm{Pr}\beta}{1+\mathrm{R_n Pr}}\right), \tag{17}$$

$$\mathcal{H}(\vartheta,\tilde{q}) = (1-\acute{q})(L_2(\vartheta) - L_2(\overline{\vartheta}_0)) + \acute{q}\left(L_2(\vartheta) + \frac{N_t}{N_b}\left(\frac{\partial^2\Theta}{\partial y^2}\right) - \gamma\vartheta\right),. \tag{18}$$

And the initial guess and linear operators for the Eq. (16) to Eq. (18) are defined as

$$\overline{w}_0 = \frac{\cosh \mathrm{N}^2 y - \cosh \mathrm{N}^2 h}{\cosh \mathrm{N}^2 h}, \tag{19}$$

$$\overline{\vartheta}_0 = \overline{\Theta}_0 = \frac{y}{h}. \tag{20}$$

$$L_1 = \frac{\partial^2}{\partial y^2} - M^2 - \frac{1}{k}, \tag{21}$$

$$L_2 = \frac{\partial^2}{\partial y^2}, \tag{22}$$

Defining the following expansion

$$\vartheta(x,y) = \vartheta_0(x,y) + \acute{q}\vartheta_1(x,y) + \acute{q}^2\vartheta_2(x,y) + \cdots, \tag{23}$$

$$\Theta(x,y) = \Psi_0(x,y) + \acute{q}\Psi_1(x,y) + \acute{q}^2\Psi_2(x,y) + \cdots, \tag{24}$$

$$w(x,y) = w_0(x,y) + \acute{q}w_1(x,y) + \acute{q}^2 w_2(x,y) + \cdots, \tag{25}$$

Using the expensing series defined in term of ($\vartheta(x,y)$,($\Theta(x,y)$ and ($w(x,y)$) as mentioned in Eq. (23) to Eq. (25) into the Eq. (16) to Eq. (18) . We get a system of linear differential equations with their relevant boundary conditions. By comparing the powers of $\acute{q}$. Apply the scheme of HPM, we obtained the solution as $\acute{q} \rightarrow 1$, we get the required solution of temperature distribution, velocity profile, and concentration profile obtained.

4. Results and Discussion

In this section the obtained results have been discussed. It depicts from Fig. (2) that for higher values of N_b and N_t Temperature profile increases. Because the Brownian motion creates micro- mixing which rises thermal conductivity. It is observed from Fig. (3) that pressure rise shows completely opposite behavior for the various values of thermal Grashof parameter Gr_T and Basic density Grashof number Gr_F. It can conclude from the Fig. (4a) that pressure rise reducing for the larger values of magnetic parameter M. Which shows the fact that pressure can be control by using the suitable magnetic field. Also, it is concluded from this figure that flow can pass easily without imposing higher pressure inside the channel. After analysis the Fig. (4b) of to Fig. (5), it is observed that there is completely opposite behavior of friction force for the different values of the same physical parameters as compared to pressure rise distribution.

From Table 1, the R-square Entropy generation for various values of magnetic parameter *M* is 0.809, meaning that approximately 81% of the variability of Entropy generation is explained by the parameter *M* in the model while adjusted R-square 0.799 indicates that about 80% of the variability of Entropy generation is accounted for Magnetic parameter *M* by the Model. Entropy generation values for Brownian motion parameter N_b is 0.998 which indicates that approximately 99% of the variability of Entropy is due to the parameter N_b in the model while, adjusted R-square 0.999 indicates that about 99% of the variability of Entropy is accounted for N_b by the Model. In the R-square the values of Entropy generation for the parameter Thermophoresis parameter N_t is 0.403 which reveals that approximately 40% of the variability of Entropy is explained by the parameter N_t in the model while adjusted R-square 0.370 indicates that about 37% of the variability of Entropy is accounted for N_t by the Model and the Entropy values for different values of B_r is 1.00 and that 100% of the variability of Entropy is accounted for the parameter B_r in the model while adjusted ,R-square 1.00 indicates that about 100% of the variability of Entropy is accounted for B_r by the Model.

It can be concluded from the Table 2 that a decrease of -2.562 in Entropy for independent variable M, an increase of 2.029 in Entropy for N_b. Similarly, an increase of 6.307 in Entropy for the parameter N_t and increase of 68.492 in Entropy for B_r scores for every one-unit increase in *Iv*, assuming all other variables in the model as constant. Table 3 is plotted to analyze the correlation of entropy generation for some sensitive parameters. It is concluded from these results that a significant perfect positive correlation exists between Brinkman number B_r and its entropy. Strong positive relationship has been observed from the correlation results between the entropy and the parameters N_t and N_b. There is a significant very strong negative correlation exist between *M* and its entropy.

5. Conclusions

The Following outcomes demonstrated through this study are as:

- Temperature profile increases for higher values of N_b and N_t.
- Pressure distribution and Friction force has opposite behavior for larger values of the magnetic parameter, Brownian motion parameter and the thermophoresis parameter.
- The variability of entropy generation is 81% for the values of *M* while 99% variability for the parameter N_b.
- The variability of entropy generation is 40% for the values of N_t while 100% variability for the parameter B_r.

Table 1: Model Summary

Model	R	R Square	Adjusted R Square	Std. Error of the Estimate
1	.900[a]	.809	.799	.7558884
2	.999[a]	.998	.998	.0550427
3	.635[a]	.403	.370	4.6675041
4	1.000[a]	1.000	1.000	.19437519

Table 2. Coefficients

Model		Unstandardized Coefficients B	Unstandardized Coefficients Std. Error	Standardized Coefficients Beta	t	Sig.
1	(Constant)	74.223	.351		211.381	.000
	M	-2.562	.293	-.900	-8.739	.000
2	(Constant)	29.097	.026		1137.975	.000
	M	2.049	.021	.999	95.977	.000
3	(Constant)	65.565	2.168		30.239	.000
	M	6.307	1.810	.635	3.485	.003
4	(Constant)	1.359	.090		15.056	.000
	M	68.492	.075	1.000	908.676	.000

Table 3: Correlation table between entropy generation and parameters.

Entropy and Parameters	N_S Vs B_r	N_S Vs N_t	N_S Vs N_b	N_S Vs M
Values range	0.1 to 2.0	0.1 to 2.0	0.1 to 2.0	0.1 to 2.0
N	20	20	20	20
Pearson Correlation	1.000**	.635**	.999**	.900**
Sig. (2-tailed)	.000	.003	.000	.000
Remarks	Perfect Relation	Strong Positive Relation	Strong Positive Relation	Very Strong Negative Relations

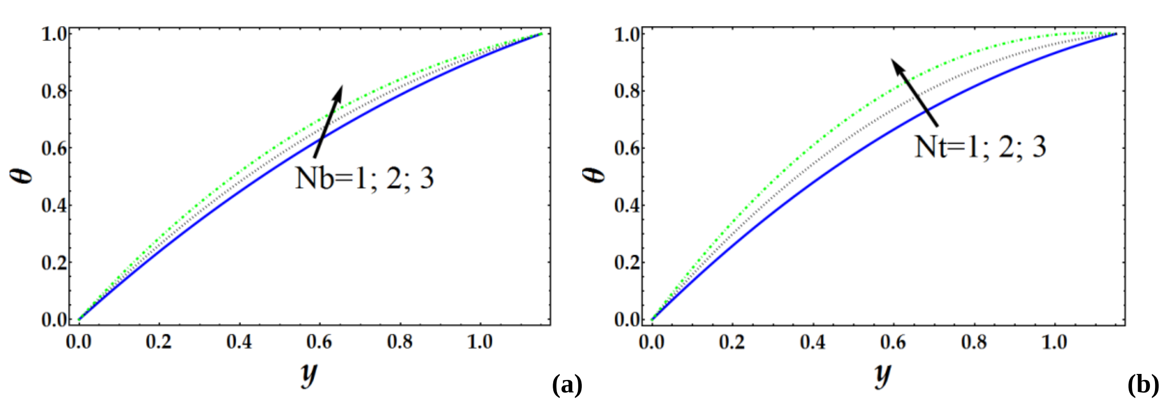

Figure 2: Temperature profile for various values of N_b and N_t when $P_r = 1, \beta = 0.8, We = 0.2, M = 0.1, Gr_T = 0.5, Gr_F = 0.6, \gamma = 0.1, k = 1$.

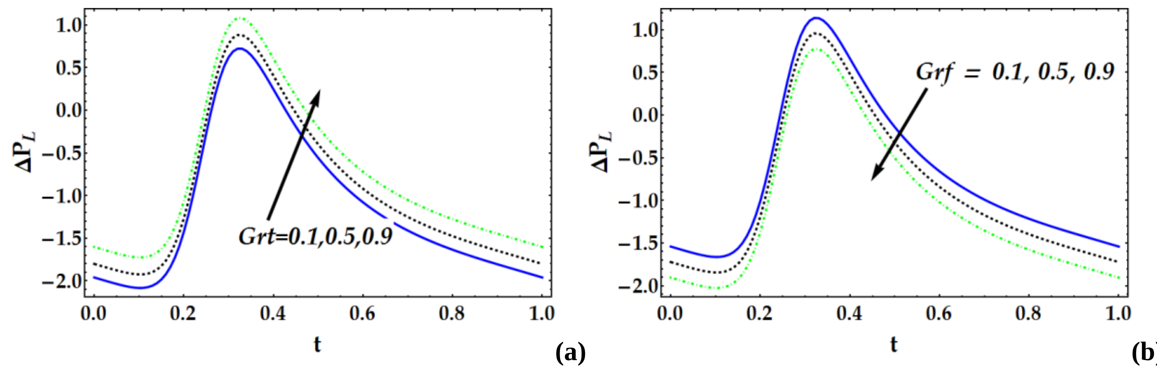

Figure 3: Pressure rise distribution for various values of Grt and G_{rf} when $N_t = 1, \beta = 0.8, We = 0.2, M = 0.1, = 0.5, \; N_b = 0.6, \; \gamma = 0.1, k = 1.$

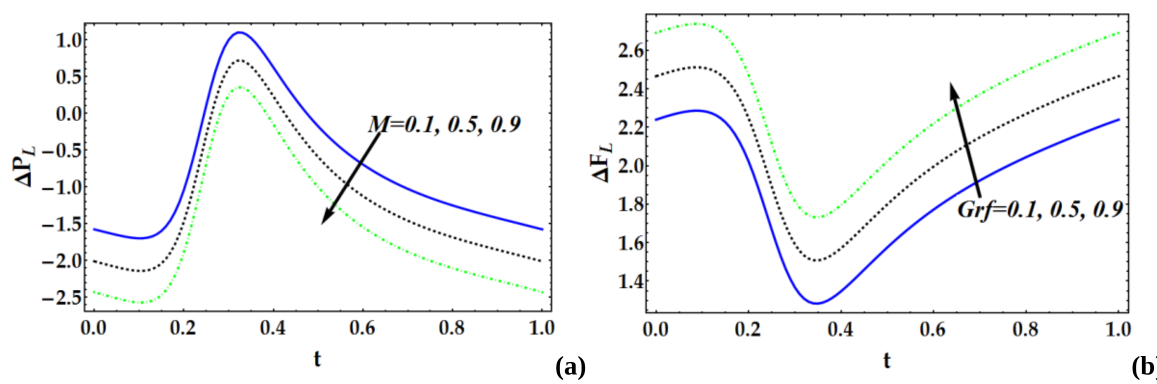

Figure 4: Pressure distribution for various values of M and Friction force profile for various values of G_{rf} when $N_t = 1, \beta = 0.8, We = 0.2, M = 0.1, Gr_T = 0.5, \gamma = 0.1, k = 1.$

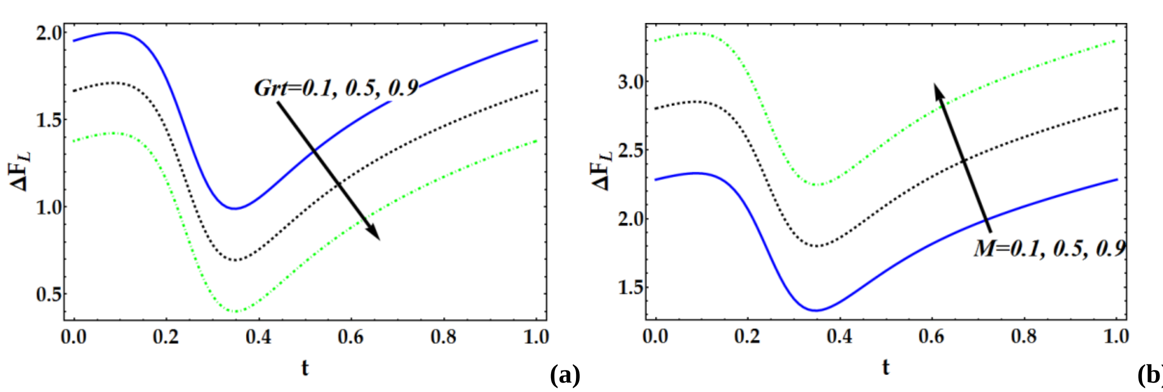

Figure 5: Friction force for various values of Gr_t and M when $N_t = 1, \beta = 0.8, We = 0.2, N_b = 0.1, \; Gr_F = 0.6, \gamma = 0.1, k = 1.$

REFERENCES

[1] S. U. S. Choi; J. A. Eastman. Enhancing thermal conductivity of fluids with nanoparticles. *Materials Science. 1995,* 231, 99-105.

[2] J. A. Eastman; U. S. Choi; S. Li, G. Soyez; L. J. Thompson; R. J. DiMelfi. Novel thermal properties of nanostructured materials. *Materials Science Forum*. 1999, 312, 629-634.

[3] Mahian, O., Kianifar, A., Heris, S. Z., Wen, D., Sahin, A. Z., & Wongwises, S. (2017). Nanofluids effects on the evaporation rate in a solar still equipped with a heat exchanger. *Nano Energy*, *36*, 134-155.

[4] Sucharitha, G., Lakshminarayana, P., & Sandeep, N. (2017). Joule heating and wall flexibility effects on the peristaltic flow of magnetohydrodynamic nanofluid. *International Journal of Mechanical Sciences*, *131*, 52-62.

[5] Mosayebidorcheh, S., & Hatami, M. (2018). Analytical investigation of peristaltic nanofluid flow and heat transfer in an asymmetric wavy wall channel (Part II: Divergent channel). *International Journal of Heat and Mass Transfer*, *126*, 800-808.

[6] Ghasemi, S. E. (2017). Thermophoresis and Brownian motion effects on peristaltic nanofluid flow for drug delivery applications. *Journal of Molecular Liquids*, *238*, 115-121.

[7] Abbas, M. A., Bai, Y., Rashidi, M. M., & Bhatti, M. M. (2016). Analysis of entropy generation in the flow of peristaltic nanofluids in channels with compliant walls. *Entropy*, *18*(3), 90.

[8] Mahian, O; Kianifar, A; Kleinstreuer, C; Moh'd A, A. N; Pop, I; Sahin, A. Z; and Wongwises. S. A review of entropy generation in Nanofluid flow. *International Journal of Heat and Mass Transfer. 2013,* 65, 514-532.

[9] M. R. AlRashidi and M. E. El-Hawary (2009), "A survey of particle swarm optimization applications in electric power systems," IEEE Transactions on Evolutionary Computation, vol. 13, no. 4, pp. 913–918.

[10] P. J. Fleming and R. C. Purshouse (2002), "Evolutionary algorithms in control systems engineering: a survey," Control Engineering Practice, vol. 10, no. 11, pp. 1223–1241.

[11] K. Ma, T. Yao, J. Yang, and X. Guan (2016), "Residential power scheduling for demand response in smart grid," International Journal of Electrical Power & Energy Systems, vol. 78, pp. 320–325.

[12] A. Zafar, S. Shah, R. Khalid, S. M. Hussain, H. Rahim, and N. Javaid (2017), "A meta-heuristic home energy management system," in 31st WAINA, pp. 244–250, IEEE.

[13] F. Merrikh-Bayat (2014), "A numerical optimization algorithm inspired by the strawberry plant," arXiv preprint arXiv:1407.7399, 2014.

[14] M. S. Asvini and T. Amudha (2016), "An efficient methodology for reservoir release optimization using plant propagation algorithm," Procedia Computer Science, vol. 93, pp. 1061–1069.

[15] [24] M. Sulaiman and A. Salhi (2015), "A seed-based plant propagation algorithm: the feeding station model," The Scientific World Journal, vol. 2015.

[16] L. Davis and S. Coombs (1987), "Genetic algorithms and communication link speed design: theoretical considerations," in Genetic algorithms and their applications: proceedings of the second International Conference on Genetic Algorithms: July 28-31, 1987 at the Massachusetts Institute of Technology, Cambridge, MA, Hills dale, NJ: L. Erlhaum Associates.

[17] D. E. Goldberg and J. H. Holland (1988), "Genetic algorithms and machine learning," Machine learning, vol. 3, no. 2, pp. 95–99.

[18] A. E. Eiben, J. E. Smith, et al. (1999), Introduction to evolutionary computing, vol. 53.Springer, 2003.

[19] C. A. C. Coello, "A comprehensive survey of evolutionary-based multiobjective optimization techniques," Knowledge and Information systems, vol. 1, no. 3,pp. 269–308.

[20] I. Fister Jr, X.-S. Yang, I. Fister, J. Brest, and D. Fister (2013), "A brief review of nature-inspired algorithms for optimization," arXiv preprint arXiv:1307.4186.

[21] X.-S. Yang and N.-I. M. Algorithms (2008), "Luniver press," Beckington, UK, pp. 242–246.

[22] H. Mu¨hlenbein, M. Schomisch, and J. Born (1991), “The parallel genetic algorithm as function optimizer,” Parallel computing, vol. 17, no. 6-7, pp. 619–632.

[23] A. To¨rn and A. Zilinskas (1989), “Global optimization (or lecture notes in computer science; vol. 350)”.